Inorganic Chemistry

Article

pubs.acs.org/IC

# Order−Disorder Transition Involving the A-Site Cations in $Ln^{3+}Mn_3V_4O_{12}$ Perovskites

Yuichi Shimakawa,*[,†,‡] Shoubao Zhang,[†] Takashi Saito,[†] Michael W. Lufaso,[§] and Patrick M. Woodward[∥]

[†]Institute for Chemical Research, Kyoto University, Uji, Kyoto 611-0011, Japan

[‡]Japan Science and Technology Agency, CREST, Uji, Kyoto 611-0011, Japan

[§]Department of Chemistry, University of North Florida, 1 UNF Drive, Jacksonville, Florida 32224, United States

[∥]Department of Chemistry, The Ohio State University, 100 West 18th Avenue, Columbus, Ohio 43210, United States

Supporting Information

**ABSTRACT:** A crossover from the A-site-ordered double-perovskite structure with $Im\bar{3}$ cubic symmetry to the simple-perovskite structure with *Pnma* orthorhombic symmetry is found in $LnMn_3V_4O_{12}$ (*Ln* = La, Nd, Gd, Y, Lu) synthesized under high-pressure conditions. Relatively large $Ln^{3+}$ ions ($La^{3+}$, $Nd^{3+}$, and $Gd^{3+}$) induce the $a^+a^+a^+$ in-phase cooperative tilting of the $VO_6$ octahedra, resulting in the A-site-ordered double-perovskite structure with chemical composition $Ln^{3+}Mn^{2+}{}_3V^{3.75+}{}_4O_{12}$. Compounds with small $Ln^{3+}$ ions like $Y^{3+}$ and $Lu^{3+}$, on the other hand, crystallize with the *Pnma* simple-perovskite structure with chemical composition $(Ln^{3+}{}_{1/4}Mn^{2+}{}_{3/4})$-$V^{3.75+}O_3$, where the $Ln^{3+}$ and $Mn^{2+}$ ions are disordered at the A site. The random distribution of the small A-site cation induces the $a^-b^+a^-$ tilting distortion of the $VO_6$ octahedra. The observed phase crossover is well explained by the structural stability calculation based on the bond-valence-sum model, and the most stable crystal structure gives the smallest unit-cell volume. This A-site-cation size-dependent phase transition between the A-site-ordered double-perovskite and A-site-disordered simple-perovskite structures in $LnMn_3V_4O_{12}$ is thus a result of the structural stability due to the cooperative tilting of the $VO_6$ octahedra. The $Mn^{2+}$ ions at the A′(A) site contribute local magnetic moments, whereas the $V^{3.75+}$ ions at the B site play a role in metallic conduction. The observed magnetic behaviors are consistent with the order−disorder distribution of the $Mn^{2+}$ ions at the A site, antiferromagnetism in the A-site-ordered double perovskites, and magnetic spin glass in the A-site-disordered simple perovskites.

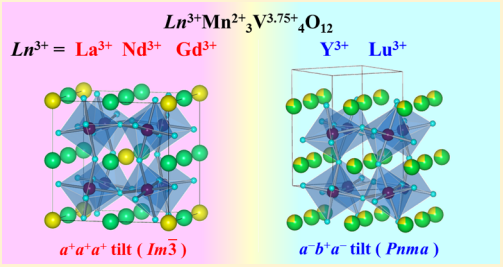


## INTRODUCTION

Perovskite is one of the most common oxide structures known. The simple-perovskite structure oxide with chemical composition $ABO_3$ is composed of a three-dimensional framework of corner-sharing $BO_6$ octahedra. Compounds with this structure show large varieties of chemical and physical properties because of interaction between the transition-metal cations at the B site and/or B−O−B interactions via oxygen ions. The A-site cavity is formed by 12 coordinated oxygen ions and usually accommodates alkali-metal ions, alkaline-earth-metal ions, and lanthanide ions. The ions at the A site play a role in tuning the properties by modifying the size of the structure and by influencing the doping states of the B-site cations.

The ideal $ABO_3$ structure is cubic, but distortions are often introduced. The most frequently seen distortion is tilting of the $BO_6$ octahedra while maintaining the rigid corner-sharing framework. This tilting is mainly driven by a mismatch between the sizes of the A-site cation and the cavity. A standard notation to describe such octahedral tilting distortions was developed by Glazer.[1,2] It describes a tilt system by rotations of the $BO_6$ octahedra about the three orthogonal Cartesian axes.

When the A-site cation is too small for the cavity, in-phase cooperative octahedral tilting of an equivalent amount about each of the three cubic axes ($a^+a^+a^+$) from the aristotype cubic perovskite ($a^0a^0a^0$) can occur, giving $Im\bar{3}$ space group symmetry. Compounds with this tilt system have the general formula $AA'_3B_4O_{12}$ and are often called an A-site-ordered double perovskite (Figure 1a). The large in-phase tilting of the $BO_6$ octahedra leads to very different coordination environments for the A and A′ sites, which are present in a 1:3 ratio. A characteristic feature of oxides with this structure is that the A′ site can also accommodate transition-metal cations. Because the transition-metal cations at both the A′ and B sites play roles in giving rise to multiple A′−A′ and A′−B interactions in addition to the B−B interaction seen in simple perovskites, further varieties of useful properties have recently been emerging in A-site-ordered $AA'_3B_4O_{12}$ compounds.[3−5] The large dielectric response over a wide temperature range found in $CaCu_3Ti_4O_{12}$ is an example.[6−8] After it was discovered, research on compounds with this structure was accelerated and led to the discoveries of large magnetoresistance in (Ca/La/Bi)-$Cu_3Mn_4O_{12}$,[9−11] multiferroic properties in $CaMn_3Mn_4O_{12}$,[12,13]

**Received:** October 31, 2013
**Published:** December 13, 2013

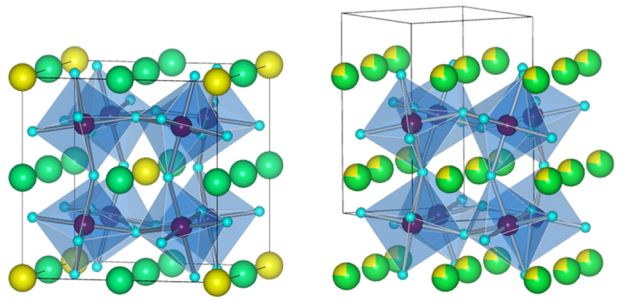


**Figure 1.** Crystal structures of (a) an A-site-ordered double perovskite ($AA'_3B_4O_{12}$) with $Im\bar{3}$ symmetry and (b) a simple perovskite ($ABO_3$) with *Pnma* symmetry. In the A-site-ordered double-perovskite structure, $a^+a^+a^+$ in-phase cooperative tilting of the octahedra gives the A and A′ sites having two different oxygen coordination environments with a 1:3 ratio. In the simple perovskite, $a^-b^+a^-$ cooperative tilting of the octahedra gives the distorted orthorhombic structure.

and large negative thermal expansion due to intersite charge transfer in $LaCu_3Fe_4O_{12}$.[14,15]

In the A-site-ordered double-perovskite structure, the A′ cations are on square-planar units that align perpendicularly to each other. Jahn–Teller active ions such as $Cu^{2+}$ and $Mn^{3+}$ are well adapted for this coordination environment, as is typically seen in $CaCu^{2+}{}_3Ti^{4+}{}_4O_{12}$ and $YMn^{3+}{}_3Al^{3+}{}_4O_{12}$.[6,16] Recent studies, however, have revealed that not only Jahn–Teller active ions $Cu^{2+}$ and $Mn^{3+}$ but also cations with other ionic states can be stabilized at the A′ sites in the A-site-ordered perovskite-structure compounds. In $ACu_3V_4O_{12}$ (A = $Na^+$, $Ca^{2+}$, $Y^{3+}$), for example, electrons are doped into both A′-site Cu and B-site V ions when a monovalent ion at the A site is replaced by a divalent or trivalent one. The doped electrons are itinerant, and the compounds show Pauli paramagnetic and metallic behaviors.[17] In $AMn_3V_4O_{12}$ (A = $Na^+$, $Ca^{2+}$, $La^{3+}$), similar aliovalent A-site substitution modulates the valence states of Mn ions at the A′ site and V ions at the B site sequentially as the valence distribution changes from $Na^+Mn^{2.33+}{}_3V^{4+}{}_4O_{12}$ to $Ca^{2+}Mn^{2+}{}_3V^{4+}{}_4O_{12}$ to $La^{3+}Mn^{2+}{}_3V^{3.75+}{}_4O_{12}$.[18] These findings of the valence-variable ions at both A′ and B sites motivate us to explore the possibility of charge transfer between the A′- and B-site ions by chemical pressure.

We here focus on $Ln^{3+}Mn_3V_4O_{12}$ with $Ln^{3+}$ ions of different sizes at the A site. Instead of seeing the charge transfer that we expected, however, we find an unusual A-site order–disorder phase transition in the perovskite structure depending on the size of the A-site $Ln^{3+}$ ion. The disordered phase adapts a *Pnma* orthorhombic structure with $a^-b^+a^-$ tilting distortion (Figure 1b), which is usually referred to as $GdFeO_3$-type distortion and is the most frequently seen in simple perovskites like the mineral $CaTiO_3$.[19] We show that the phase transition from the A-site-ordered double perovskite to the A-site-disordered simple perovskite in $Ln^{3+}Mn_3V_4O_{12}$ is due to the structural stability associated with the cooperative tilting of the $BO_6$ octahedra.

## EXPERIMENTAL SECTION

Polycrystalline samples of $LaMn_3V_4O_{12}$, $NdMn_3V_4O_{12}$, $GdMn_3V_4O_{12}$, $YMn_3V_4O_{12}$, and $LuMn_3V_4O_{12}$ were prepared by solid-state reactions under high-pressure and high-temperature conditions by using a cubic-anvil-type high-pressure apparatus.[4] Stoichiometric amounts of raw materials, $Ln_2O_3$ (*Ln* = La, Nd, Gd, Y, Lu), $Mn_2O_3$, $V_2O_3$, and $V_2O_5$, were well mixed, sealed into gold capsules, treated at 9 GPa and 900 °C for 30 min, and then cooled to room temperature before the pressure was released.

Synchrotron X-ray diffraction (XRD) experiments at room temperature were performed for phase identification and structural analysis. Diffraction patterns with wavelengths of 0.499959 Å for $LaMn_3V_4O_{12}$, 0.598704 Å for $NdMn_3V_4O_{12}$, and 0.598411 Å for $GdMn_3V_4O_{12}$, $YMn_3V_4O_{12}$, and $LuMn_3V_4O_{12}$ were collected with a large Debye–Scherrer camera installed at BL19B2 in SPring-8. The crystal structures were analyzed by the Rietveld method with the program *RIETAN-2000*.[20]

The structural stabilities of the compounds were evaluated using the program *SPuDS*.[21,22] The program gives the size of the octahedron and the optimum magnitude of the octahedral tilt angle based on the bond-valence-sum (BVS) model.[23,24] The calculated structure is one in which the difference between the calculated BVS and formal valence for each ion is minimized. The structural stability of a compound with a given composition was evaluated by comparing the quantity, referred to as the global instability index (GII), which is equal to $\{[\sum_i [V_i(\mathrm{OX}) - V_i(\mathrm{calc})]^2]/N\}^{1/2}$, where $N$ is the number of atoms in the formula unit and $V_i$(OX) and $V_i$(calc) are respectively the formal valence and calculated BVS for the $i$th ion. The B–O distance is fixed to a value to give $V_B$(calc) = $V_B$(OX), while the lattice parameters as well as the fractional coordinates of oxygen are optimized so as to minimize GII. Previous studies have shown that *SPuDS* can make useful predictions of the structural stability of perovskites and be used to guide the high-pressure synthesis of these phases.[25−28] The formal valences of the constituent ions of $LnMn_3V_4O_{12}$ were set to $Ln^{3+}$, $Mn^{2+}$, $V^{3.75+}$, and $O^{2-}$, as we clarified in a previous study for $La^{3+}Mn^{2+}{}_3V^{3.75+}{}_4O_{12}$.[18] For the mixed-valence state of $V^{3.75+}$ at the B site, we used a weighted $r_0$ (1.774) as an average of $1/4r_0(V^{3+})$ and $3/4r_0(V^{4+})$.

Resistivity of the samples was measured by a standard four-probe method. The magnetic susceptibility with 1 and 10 kOe external magnetic fields was also measured between 5 and 300 K in zero-field-cooled (ZFC) and field-cooled (FC) modes.

## RESULTS AND DISCUSSION

Figure 2 shows synchrotron XRD patterns of the synthesized samples. All samples are single phases with no apparent impurity phases. $LaMn_3V_4O_{12}$, $NdMn_3V_4O_{12}$, and $GdMn_3V_4O_{12}$ have quite similar diffraction patterns and crystallize with the A-site-ordered double-perovskite structure having $Im\bar{3}$ cubic symmetry. The result of structure refinement

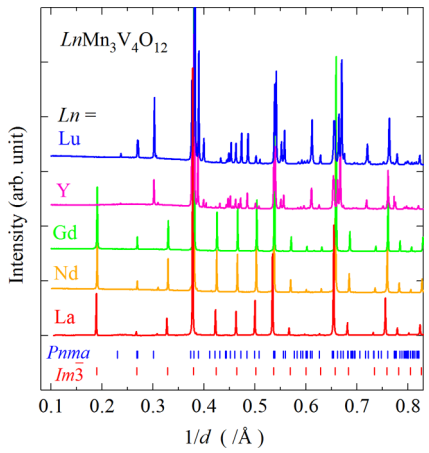


**Figure 2.** Synchrotron XRD patterns of $LnMn_3V_4O_{12}$ (*Ln* = La, Nd, Gd, Y, Lu). The ticks at the bottom indicate the positions of the Bragg reflections from the $Im\bar{3}$ cubic and *Pnma* orthorhombic structures.


dx.doi.org/10.1021/ic402740k | *Inorg. Chem.* 2014, 53, 594–599

for $LaMn_3V_4O_{12}$ is shown in Figure 3a as an example. The refined structure parameters for the three samples are listed in Table 1 and the Supporting Information (Figures S1–S3 and Tables S1–S3). For $LaMn_3V_4O_{12}$, 4 of the 12 Mn–O distances are quite short, 2.124(3) Å, and the other 8 are either 2.751(3) or 3.168(3) Å, making the nearly square-planar unit. This coordination environment for the A′-site Mn gives a BVS of 2.02. The 12 La–O distances, 2.642(3) Å, give a BVS of 3.37 for La at the A site. The V–O distance in the octahedron is 1.943(1) Å, giving a BVS of 3.80. Because no apparent vacancies were seen at any of the sites in the structure refinement, the result suggests that the charge distribution of the compound is $La^{3+}Mn^{2+}{}_3V^{3.75+}{}_4O_{12}$, which was also confirmed by spectroscopy measurements.[18] Note that this charge distribution is the same as those of $La^{3+}Cu^{2+}{}_3Mn^{3.75+}{}_4O_{12}$ and $La^{3+}Cu^{2+}{}_3Fe^{3.75+}{}_4O_{12}$[10,14] but is different from that of $Ln^{3+}{}_{2/3}Cu^{2+}{}_3Ti^{4+}{}_4O_{12}$, where one-third of the *Ln* sites are vacant.[5,29] Actually, when we refine the crystal structure, the A-site occupancy always converges to a value close to 1.0 (or more than 1.0), suggesting full occupation of this site. The crystal structures of $NdMn_3V_4O_{12}$ and $GdMn_3V_4O_{12}$ are quite similar to that of $LaMn_3V_4O_{12}$, and thus the A-site-ordered double-perovskite structures of $Ln^{3+}Mn^{2+}{}_3V^{3.75+}{}_4O_{12}$ (*Ln* = La, Nd, Gd) include the $a^+a^+a^+$ in-phase cooperative tilting of the $VO_6$ octahedra shown in Figure 1a.

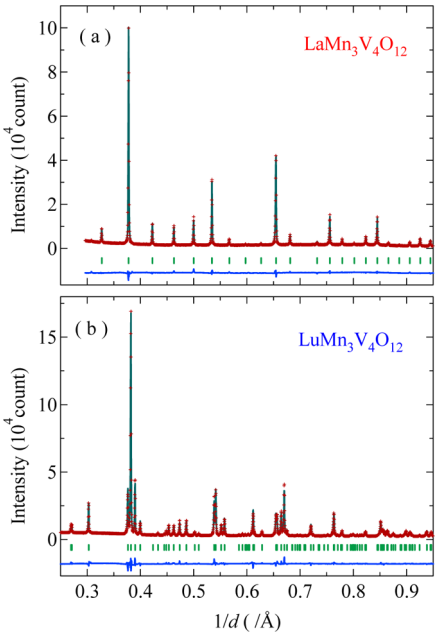


**Figure 3.** Synchrotron XRD patterns and structure refinement results for (a) A-site-ordered double-perovskite $LaMn_3V_4O_{12}$ and (b) A-site-disordered simple-perovskite $LuMn_3V_4O_{12}$ [$(Lu_{1/4}Mn_{3/4})VO_3$]. The observed (marks), calculated (line), and difference (bottom line) patterns are shown. The ticks indicate the positions of the Bragg reflections.

The synchrotron XRD patterns of $YMn_3V_4O_{12}$ and $LuMn_3V_4O_{12}$ (Figure 2), on the other hand, are rather different from those of the above $LnMn_3V_4O_{12}$ (*Ln* = La, Nd, Gd), and they are well reproduced with a $GdFeO_3$-type distorted simple-perovskite structure model with *Pnma* symmetry. The result of structure refinement for $LuMn_3V_4O_{12}$ is shown in Figure 3b, and the refined structure parameters for $YMn_3V_4O_{12}$ and $LuMn_3V_4O_{12}$ are also listed in Table 1 and the Supporting Information (Figures S4 and S5 and Tables S4 and S5). The distorted 12-fold-coordinated A site (4c Wyckoff atomic position) in the perovskite structure is occupied by both *Ln*

**Table 1. Refined Structure Parameters, Selected Bond Lengths, and Calculated BVS Values for $LnMn_3V_4O_{12}$ (*Ln* = La, Nd, Gd, Y, Lu) from Rietveld Analysis of Synchrotron XRD Data[a]**

| $Ln^{3+}$ | $La^{3+}$ | $Nd^{3+}$ | $Gd^{3+}$ | | $Y^{3+}$ | $Lu^{3+}$ |
|---|---|---|---|---|---|---|
| ionic radius (Å) | 1.160 | 1.109 | 1.053 | | 1.019 | 0.977 |
| space group | $Im\bar{3}$ | $Im\bar{3}$ | $Im\bar{3}$ | | *Pnma* | *Pnma* |
| *a* (Å) | 7.4830(1) | 7.4596(1) | 7.4403(1) | | 5.3328(2) | 5.3250(1) |
| *b* (Å) | | | | | 7.4624(3) | 7.4396(2) |
| *c* (Å) | | | | | 5.1667(2) | 5.1415(1) |
| *V* (Å$^3$) | 419.01(1) | 415.10(1) | 411.88(1) | | 411.61(2)[b] | 407.38(2)[b] |
| $R_{wp}$ (%) | 4.96 | 4.94 | 6.19 | | 3.14 | 4.30 |
| $R_p$ (%) | 3.87 | 3.35 | 4.51 | | 1.91 | 3.19 |
| Mn–O (Å) | 2.124(3) × 4 | 2.125(1) × 4 | 2.135(2) × 4 | Mn/*Ln*–O (Å) | 2.136(5) | 2.143(4) |
| | 2.751(3) × 4 | 2.773(2) × 4 | 2.794(3) × 4 | | 2.224(5) | 2.194(5) |
| | 3.168(3) × 4 | 3.153(1) × 4 | 3.132(2) × 4 | | 2.222(4) × 2 | 2.204(4) × 2 |
| *Ln*–O (Å) | 2.642(3) × 12 | 2.601(2) × 12 | 2.561(3) × 12 | | 2.481(4) × 2 | 2.466(4) × 2 |
| | | | | | 2.622(4) × 2 | 2.603(4) × 2 |
| | | | | | 3.145(5) | 3.127(4) |
| | | | | | 3.263(5) | 3.294(5) |
| | | | | | 3.360(4) × 2 | 3.396(4) × 2 |
| BVS for Mn | 2.02 | 2.00 | 1.95 | | 1.92 | 1.99 |
| BVS for *Ln* | 3.37 | 3.14 | 3.14 | | 3.56 | 3.24 |
| V–O (Å) | 1.943(1) × 6 | 1.936(2) × 6 | 1.929(3) × 6 | | 1.903(4) × 2 | 1.920(4) × 2 |
| | | | | | 1.969(4) × 2 | 1.952(4) × 2 |
| | | | | | 1.968(2) × 2 | 1.963(1) × 2 |
| BVS for V | 3.80 | 3.87 | 3.95 | | 3.78 | 3.78 |

[a]The numbers in parentheses are standard deviations of the last significant digit. [b]The unit-cell volumes for orthorhombic $YMn_3V_4O_{12}$ and $LuMn_3V_4O_{12}$ are doubled for comparison.


dx.doi.org/10.1021/ic402740k | *Inorg. Chem.* 2014, 53, 594–599

and Mn ions in the ratio 1:3. No apparent oxygen vacancies are also detected in the structure refinements. For $LuMn_3V_4O_{12}$, the BVS for Mn at the A site is 1.99, and that for Lu in the same environment is 3.24. The V−O distances in the octahedron are 1.920(4), 1.952(4), and 1.963(1) Å, giving a BVS of 3.78. The result of structure refinement for $YMn_3V_4O_{12}$ is essentially the same, and thus given the stoichiometric composition, the compounds can be described as simple perovskites $(Y^{3+}{}_{1/4}Mn^{2+}{}_{3/4})V^{3.75+}O_3$ and $(Lu^{3+}{}_{1/4}Mn^{2+}{}_{3/4})V^{3.75+}O_3$.

It is interesting to note that in the orthorhombic structures of $YMn_3V_4O_{12}$ and $LuMn_3V_4O_{12}$ the four shortest Mn/*Ln*−O distances are of lengths very similar to the short Mn−O distances in the cubic structures of the $LnMn_3V_4O_{12}$ (*Ln* = La, Nd, Gd) compounds. What has apparently changed is the fact that the $Ln^{3+}$ ion is now small enough to squeeze into the same site that $Mn^{2+}$ occupies, as evidenced by the fact that the BVS for $Lu^{3+}$ is not that far above its ideal value of 3. Once the driving force for an ordered distribution of $Ln^{3+}$ and $Mn^{2+}$ ions is lost, the $a^+a^+a^+$ tilting is no longer favored and $a^-b^+a^-$ tilting of the $VO_6$ octahedra occurs, as shown in Figure 1b. Because a perovskite $MnVO_3$, where the A site is fully occupied by the transition-metal cation $Mn^{2+}$, was recently reported to be synthesized with the high-pressure technique,[30] the present compounds with the A-site partially occupied by $Mn^{2+}$ appear to be reasonable. $(Ln^{3+}{}_{1/4}Mn^{2+}{}_{3/4})V^{3.75+}O_3$ (*Ln* = Y, Lu) can be a phase in solid solutions of $MnVO_3$ and $LnVO_3$.

Because the ionic radius of $Ln^{3+}$ ions decreases from 1.160 Å for $La^{3+}$ to 1.109 Å for $Nd^{3+}$ to 1.053 Å for $Gd^{3+}$ to 1.019 Å for $Y^{3+}$ to 0.977 Å for $Lu^{3+}$,[31,32] one can infer that a relatively large A-site cation stabilizes the $Im\bar{3}$ A-site-ordered double-perovskite structure, while a relatively small A-site one stabilizes the *Pnma* orthorhombic simple-perovskite structure. The cooperative tilting of the $VO_6$ octahedra thus changes from $a^+a^+a^+$ to $a^-b^+a^-$ with decreasing size of the A-site cation. This phase change between the A-site-ordered double perovskite and the disordered simple perovskite is well reproduced by the structural stability calculation by *SPuDS*. The GII values calculated for the $Im\bar{3}$ A-site-ordered double perovskites $Ln^{3+}Mn^{2+}{}_3V^{3.75+}{}_4O_{12}$ and the *Pnma* simple perovskites $(Ln^{3+}{}_{1/4}Mn^{2+}{}_{3/4})V^{3.75+}O_3$ (*Ln* = La, Nd, Gd, Y, Lu) are shown in Figure 4a. It is interesting to note that, for a compound with $Gd^{3+}$, $Nd^{3+}$, or $La^{3+}$, the GII for the $Im\bar{3}$ A-site-ordered structure is lower than that for the *Pnma* structure, predicting that for compounds with relatively large cations at the A site, the $Im\bar{3}$ A-site-ordered double-perovskite structure is more stable than the *Pnma* simple-perovskite structure. In contrast, GII(*Pnma*) is lower than GII($Im\bar{3}$) for the small A-site ions of $Lu^{3+}$ and $Y^{3+}$. A crossover in the stable structure from the $Im\bar{3}$ A-site-ordered double-perovskite phase to the *Pnma* simple-perovskite phase takes place at the A-site ion size around 1.03 Å, and the $a^+a^+a^+$ tilting of the $VO_6$ octahedra changes to $a^-b^+a^-$. A-site ions like $Y^{3+}$ and $Lu^{3+}$ are too small to stabilize the in-phase cooperative tilting of the $VO_6$ octahedra. Actually, the *SPuDS* calculation for the $Im\bar{3}$ cubic $Lu^{3+}Mn^{2+}{}_3V^{3.75+}{}_4O_{12}$ structure predicts a BVS for $Lu^{3+}$ of 1.96, which is far from the ideal value of 3 and is substantially smaller than 2.76 for $La^{3+}$ in the cubic $La^{3+}Mn^{2+}{}_3V^{3.75+}{}_4O_{12}$. Because the $a^+a^+a^+$ tilting gives two very different sites for A and A′, the stability of the $Im\bar{3}$ cubic structure should disappear altogether when the $Ln^{3+}$ ion at the A site has a radius similar to that of the $Mn^{2+}$ ion (0.96 Å)[32] at the A′ site. Note also that the $a^-b^+a^-$ tilting of the octahedra induces disorder of the $Ln^{3+}$ and $Mn^{2+}$ ions at the A site. An order−disorder phase change like this has never been

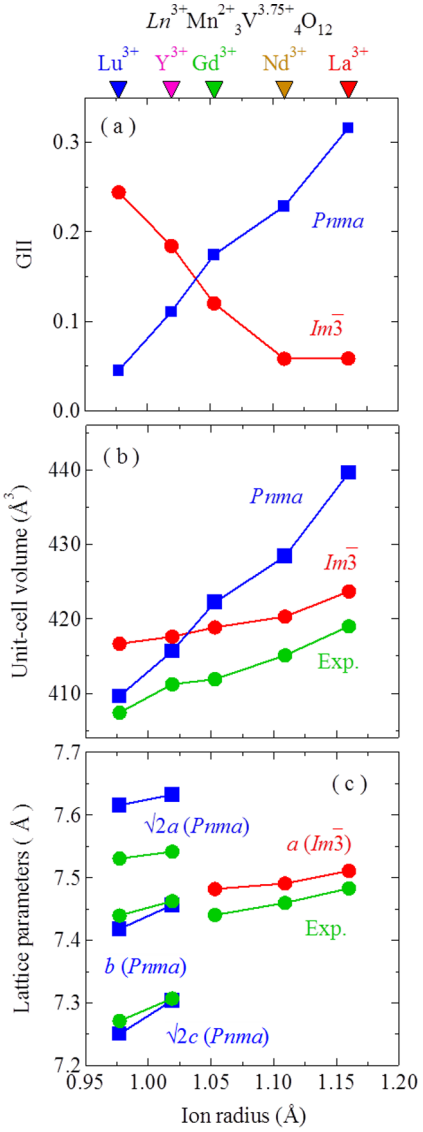


**Figure 4.** (a) Calculated GII and (b) unit-cell volume (for $LnMn_3V_4O_{12}$ unit) as a function of the A-site $Ln^{3+}$ ion radius. Unit-cell volumes obtained experimentally by structure analysis are also plotted in part b. (c) Lattice parameters predicted by the *SPuDS* calculations and obtained from structure analysis are plotted as a function of the A-site $Ln^{3+}$ ion radius.

observed in a similar series of compounds. All $Ln^{3+}{}_{2/3}Cu^{2+}{}_3Ti^{4+}{}_4O_{12}$ compounds with *Ln* from large $La^{3+}$ to small $Lu^{3+}$ crystallize with the A-site-ordered double-perovskite structure (see also the Supporting Information, Figure S6).[5,29] $Ln^{3+}Mn^{3+}{}_3Al^{3+}{}_4O_{12}$ compounds with small A-site cations such as $Yb^{3+}$, $Y^{3+}$, and $Dy^{3+}$ crystallize with the A-site-ordered double-perovskite structure, but $La^{3+}Mn^{3+}{}_3Al^{3+}{}_4O_{12}$ with the large A-site cation could not be synthesized as a single phase.[33]

Interestingly, as shown in Figure 4b, for $LnMn_3V_4O_{12}$ (*Ln* = La, Nd, Gd) with GII($Im\bar{3}$) < GII(*Pnma*), the calculated unit-cell volume of the A-site-ordered structure ($Im\bar{3}$) is smaller than that of the disordered simple-perovskite structure (*Pnma*), while for $LnMn_3V_4O_{12}$ (*Ln* = Y, Lu) with GII(*Pnma*) < GII($Im\bar{3}$), the unit-cell volume of the disordered perovskite structure (*Pnma*) is smaller than that of the A-site-ordered double-perovskite structure ($Im\bar{3}$). The stable crystal structure, which is predicted as the one with the lowest GII, has the


dx.doi.org/10.1021/ic402740k | Inorg. Chem. 2014, 53, 594−599

smaller unit-cell volume. Furthermore, the predicted unit-cell volume of $LnMn_3V_4O_{12}$ agrees quite well with the one obtained experimentally. Note also that the unit-cell volume decreases with decreasing size of the A-site cation from $La^{3+}$ to $Lu^{3+}$ even when the crystal structure changes from A-site-ordered $Im\bar{3}$ cubic to A-site-disordered *Pnma* orthorhombic. The lattice parameters of both the A-site-ordered $Im\bar{3}$ cubic double-perovskite and disordered *Pnma* orthorhombic simple-perovskite structures are also well reproduced by the *SPuDS* calculation (Figure 4c).

As we reported previously,[18] Mn at the A′ site in $LaMn_3V_4O_{12}$ gives local magnetic moments, whereas V at the B site plays a role in metallic conduction. Thus, the electrons of the A′-site Mn are localized, while those of the B-site V are delocalized. The magnetic and transport behaviors of other $LnMn_3V_4O_{12}$ are similar to those of $LaMn_3V_4O_{12}$ (Supporting Information, Figures S7 and S8). All samples show very low resistivity at room temperature, suggesting delocalization of the electrons. All samples show paramagnetic susceptibilities at temperatures above about 100 K, and some show magnetic orderings at low temperatures, confirming the presence of the local magnetic moments. The temperature dependence of the magnetic susceptibility is shown for $LaMn_3V_4O_{12}$ and $LuMn_3V_4O_{12}$ in Figure 5. Because both $La^{3+}$ and $Lu^{3+}$ are

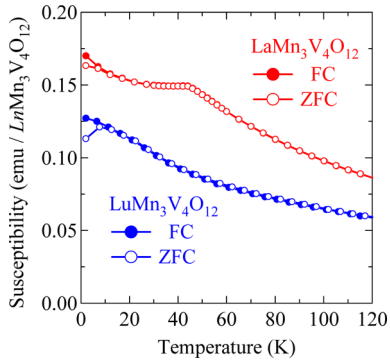


**Figure 5.** Temperature dependence of the magnetic susceptibility measured under ZFC (open symbols) and FC (closed symbols) for A-site-ordered double perovskite $LaMn_3V_4O_{12}$ and A-site-disordered simple perovskite $LuMn_3V_4O_{12}$.

nonmagnetic, only $Mn^{2+}$ at the A site contributes to the magnetic behaviors. The susceptibilites above 100 K for both compounds indeed obey the Curie–Weiss law, as shown in Figure 6, and the Curie constants obtained by the fit to the experimental data are 12.75 emu·K/mol for $LaMn_3V_4O_{12}$ and 12.32 emu·K/mol for $LuMn_3V_4O_{12}$, indicating the contribution of $Mn^{2+}$ ($S = {}^5/_2$) local moments (the expected Curie constant, 13.13 emu·K/mol) to the magnetic properties. In contrast to a clear antiferromagnetic transition at 45 K for $LaMn_3V_4O_{12}$, a spin-glass-like magnetic behavior, in which the susceptibility shows hysteresis under ZFC and FC measurements, is observed for $LuMn_3V_4O_{12}$ below about 10 K. In the A-site-ordered double-perovskite $LaMn_3V_4O_{12}$, antiferromagnetic interaction between the nearest-neighbor $Mn^{2+}$ spin ($S = {}^5/_2$) located at the A′ site makes an antiferromagnetic spin structure below the transition temperature. In $LuMn_3V_4O_{12}$ [$(Lu_{1/4}Mn_{3/4})VO_3$], on the other hand, random distribution of the $Mn^{2+}$ ions at the A site in the perovskite structure prevents the spins of $Mn^{2+}$ from making a long-range ordering, resulting in the spin-glass-like magnetic state. Indeed, the Weiss temperature of $LuMn_3V_4O_{12}$

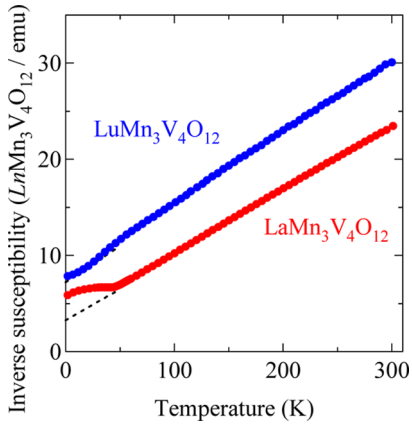


**Figure 6.** Temperature dependence of the inverse susceptibility for $LaMn_3V_4O_{12}$ and $LuMn_3V_4O_{12}$.

obtained from the Curie–Weiss fit is about −90 K, which is much higher than the spin-glass-like magnetic transition temperature of 10 K. The second- or third-nearest longer-range magnetic interaction of the randomly distributed $Mn^{2+}$ ions in the A-site spin sublattice plays a role in the spin-glass-like magnetic behavior.

Again, in the present results, we cannot see any significant discrepancies from the formal charge distribution of $Ln^{3+}Mn^{2+}{}_3V^{3.75+}{}_4O_{12}$ [$(Ln^{3+}{}_{1/4}Mn^{2+}{}_{3/4})V^{3.75+}O_3$]. In spite of the chemical pressure exerted by changing the size of the A-site ion, no apparent charge changes, e.g., intersite charge transfer between the A′-site Mn and B-site V ions, are evident. In the $LnMn_3V_4O_{12}$ system, therefore, the size of the A-site cation simply affects the structural stability and modifies the cooperative tilting of the $VO_6$ octahedra to fit the A-site ion to the A-site cavity. An important point is that the structure change is also associated with the order–disorder transition of the cations at the A site in the perovskite structure.

## CONCLUSION

$LnMn_3V_4O_{12}$ (*Ln* = La, Nd, Gd, Y, Lu) compounds with $Ln^{3+}$ ions of different sizes were synthesized under high-pressure (9 GPa) and high-temperature (900 °C) conditions. Instead of seeing the intersite charge transfer between the valence-variable A′-site Mn and B-site V ions, we found an A-site order–disorder transition in the perovskite structures depending on the size of the A-site $Ln^{3+}$ ion. The compounds with relatively large $Ln^{3+}$ ions ($La^{3+}$, $Nd^{3+}$, and $Gd^{3+}$) crystallized with the A-site-ordered $Im\bar{3}$ double-perovskite structure $Ln^{3+}Mn^{2+}{}_3V^{3.75+}{}_4O_{12}$ with $a^+a^+a^+$ in-phase cooperative tilting of the $VO_6$ octahedra. The compounds with small $Ln^{3+}$ ions like $Y^{3+}$ and $Lu^{3+}$, on the other hand, crystallized with the *Pnma* simple-perovskite structure, where the $Ln^{3+}$ and $Mn^{2+}$ ions were disordered at the A site. The random distribution of the small A-site cation induced the $a^-b^+a^-$ tilting distortion of the $VO_6$ octahedra. The charge distribution of the synthesized compounds is $Ln^{3+}Mn^{2+}{}_3V^{3.75+}{}_4O_{12}$ [$(Ln^{3+}{}_{1/4}Mn^{2+}{}_{3/4})V^{3.75+}O_3$], and $Mn^{2+}$ at the A′ (A) site contributed local magnetic moments, whereas $V^{3.75+}$ at the B site played a role in metallic conduction. In contrast to the antiferromagnetic transitions of $Mn^{2+}$ spins in the A-site-ordered double-perovskite structure compounds, random distribution of the $Mn^{2+}$ ions at the A site in the simple-perovskite structure resulted in a spin-glass-like magnetic state.


dx.doi.org/10.1021/ic402740k | *Inorg. Chem.* 2014, 53, 594–599

The structural stability calculation by the program *SPuDS* well explained the observed phase change of the A-site-ordered double perovskite and the disordered simple perovskite. A crossover from the $Im\bar{3}$ A-site-ordered double-perovskite structure to the *Pnma* simple-perovskite structure depending on the size of the A-site $Ln^{3+}$ cation was evident when comparing the GII values for the compounds with different A-site cations. The unit-cell volumes and lattice parameters of both A-site-ordered double-perovskite and A-site-disordered simple-perovskite phases were also well predicted by the calculation. We can thus conclude that in $Ln^{3+}Mn_3V_4O_{12}$ the A-site-cation size-dependent phase transition between the A-site-ordered double-perovskite and A-site-disordered simple-perovskite structures is due to the structural stability associated with the cooperative tilting of the $VO_6$ octahedra.

The present results also demonstrate that the *SPuDS* calculations based on the BVS model provide a good indicator of not only what kind of perovskite-structure compounds can be synthesized but also which distortion can be introduced in the structure. Because the observed magnetic behaviors of antiferromagnetism and spin glass strongly depend on the ordering of the $Mn^{2+}$ ions at the A site, the results also demonstrate that those calculations can predict the properties of perovskite-structure oxide compounds.

## ■ ASSOCIATED CONTENT

### Ⓢ Supporting Information

Synchrotron XRD patterns and structure refinement results, GII calculation for hypothetical $Ln^{3+}Cu^{2+}{}_3Ti^{4+}{}_4O_{12}$, and magnetic and transport measurement results. This material is available free of charge via the Internet at http://pubs.acs.org.

## ■ AUTHOR INFORMATION


### Corresponding Author

*E-mail: shimak@scl.kyoto-u.ac.jp.


### Notes

The authors declare no competing financial interest.

## ■ ACKNOWLEDGMENTS

We thank K. Osaka and I. Hirosawa for their help with synchrotron XRD measurements at BL19B2 in SPring-8 in Japan. The experiments in SPring-8 were performed with the approval of the Japan Synchrotron Radiation Research Institute. This work was partly supported by Grants-in-Aid for Scientific Research (Grants 19GS0207 and 22740227) and by a grant for the Joint Project of Chemical Synthesis Core Research Institutions from the Ministry of Education, Culture, Sports, Science and Technology of Japan. The work was also supported by Japan Science and Technology Agency, CREST. M.W.L. thanks UNF for the Munoz Professorship.

## ■ REFERENCES


(1) Glazer, A. M. *Acta Crystallogr., Sect. B* **1972**, *28*, 3384.
(2) Glazer, A. M. *Acta Crystallogr., Sect. A* **1975**, *31*, 756.
(3) Vasil'ev, A. N.; Volkova, O. S. *Low Temp. Phys.* **2007**, *33*, 895.
(4) Shimakawa, Y. *Inorg. Chem.* **2008**, *47*, 8562.
(5) Shimakawa, Y.; Saito, T. *Phys. Status Solidi B* **2013**, *249*, 423.
(6) Subramanian, M. A.; Li, D.; Duan, N.; Reisner, B. A.; Sleight, A. W. *J. Solid State Chem.* **2000**, *151*, 323.
(7) Ramirez, A. P.; Subramanian, M. A.; Gardel, M.; Blumberg, G.; Li, D.; Vogt, T.; Shapiro, S. M. *Solid State Commun.* **2000**, *115*, 217.
(8) Homes, C. C.; Vogt, T.; Shapiro, S. M.; Wakimoto, S.; Ramirez, A. P. *Science* **2001**, *293*, 673.
(9) Zeng, Z.; Greenblatt, M.; Subramanian, M. A.; Croft, M. *Phys. Rev. Lett.* **1999**, *82*, 3164.
(10) Alonso, J. A.; Sanchez-Benitez, J.; de Andres, A.; Martinez-Lope, M. J.; Casais, M. T.; Martinez, J. L. *Appl. Phys. Lett.* **2003**, *83*, 2623.
(11) Takata, K.; Yamada, I.; Azuma, M.; Takano, M.; Shimakawa, Y. *Phys. Rev. B* **2007**, *76*, 024429.
(12) Zhang, G.; Dong, S.; Yan, Z.; Guo, Y.; Zhang, Q.; Yunoki, S.; Dagotto, E.; Liu, J.-M. *Phys. Rev. B* **2011**, *84*, 174413.
(13) Johnson, R. D.; Chapon, L. C.; Khalyavin, D. D.; Manuel, P.; Radaelli, P. G.; Martin, C. *Phys. Rev. Lett.* **2012**, *108*, 067201.
(14) Long, Y. W.; Hayashi, N.; Saito, T.; Azuma, M.; Muranaka, S.; Shimakawa, Y. *Nature* **2009**, *458*, 60.
(15) Chen, W. T.; Saito, T.; Hayashi, N.; Takano, M.; Shimakawa, Y. *Sci. Rep.* **2012**, *2*, 449.
(16) Tohyama, T.; Saito, T.; Mizumaki, M.; Agui, A.; Shimakawa, Y. *Inorg. Chem.* **2010**, *49*, 2492.
(17) Shiraki, H.; Saito, T.; Azuma, M.; Shimakawa, Y. *J. Phys. Soc. Jpn.* **2008**, *77*, 064705.
(18) Zhang, S. B.; Saito, T.; Mizumaki, M.; Chen, W.-T.; Tohyama, T.; Shimakawa, Y. *J. Am. Chem. Soc.* **2013**, *135*, 6056.
(19) Sasaki, S.; Prewitt, C. T.; Bass, J. D. *Acta Crystallogr., Sect. C* **1987**, *43*, 1668.
(20) Izumi, F.; Ikeda, T. *Mater. Sci. Forum* **2000**, *321*−*324*, 198.
(21) Lufaso, M. W.; Woodward, P. M. *Acta Crystallogr., Sect. B* **2001**, *57*, 725.
(22) Lufaso, M. W.; Barnes, P. W.; Woodward, P. M. *Acta Crystallogr., Sect. B* **2006**, *62*, 397.
(23) Brown, I. D. *Chem. Soc. Rev.* **1978**, *7*, 359.
(24) Brown, I. D.; Altermatt, D. *Acta Crystallogr., Sect. B* **1985**, *41*, 244.
(25) Byeon, S.-H.; Lufaso, M. W.; Parise, J. B.; Woodward, P. M.; Hansen, T. *Chem. Mater.* **2003**, *15*, 3798.
(26) Byeon, S.-H.; Lee, S.-S.; Parise, J. B.; Woodward, P. M.; Hur, N. H. *Chem. Mater.* **2004**, *16*, 3697.
(27) Byeon, S.-H.; Lee, S.-S.; Parise, J. B.; Woodward, P. M.; Hur, N. H. *Chem. Mater.* **2005**, *17*, 3552.
(28) Byeon, S.-H.; Lee, S.-S.; Parise, J. B.; Woodward, P. M. *Chem. Mater.* **2006**, *18*, 3873.
(29) Dittl, A.; Krohns, S.; Sebald, J.; Schrettle, F.; Hemmida, M.; von Nidda Krug, H.-A.; Riegg, S.; Reller, A.; Ebbinghaus, S. G.; Loidl, A. *Eur. Phys. J. B* **2011**, *79*, 391.
(30) Markkula, M.; Arevalo-Lopez, A. M.; Kusmartseva, A.; Rodgers, J. A.; Ritter, C.; Wu, H.; Attfield, J. P. *Phys. Rev. B* **2011**, *84*, 094450.
(31) Shannon, R. D. *Acta Crystallogr., Sect. A* **1976**, *32*, 751.
(32) Because the ionic radii of not all $Ln^{3+}$ (*Ln* = La, Nd, Gd, Y, Lu) ions for 12 oxygen coordination were known, those for 8 oxygen coordination are used in this study. Also, the ionic radius for $Mn^{2+}$ for 8 oxygen coordination is 0.96 Å. See http://abulafia.mt.ic.ac.uk/shannon/ptable.php.
(33) Saito, T.; Tohyama, T.; Woodward, P. M.; Shimakawa, Y. *Bull. Chem. Soc. Jpn.* **2011**, *84*, 802.